Random telegraph noise on the threshold voltage of multi-level flash memory*

Yiming Liao(廖轶明)[1], Xiaoli Ji(纪小丽)[1,†], Yue Xu(徐跃)[3], Chengxu Zhang(张城绪)[1], Qiang Guo(郭强)[2], and Feng Yan(闫锋)[1]

[1] College of Electronic Science and Engineering, Nanjing University, Nanjing 210093, China
[2] Quality and Reliability Engineering, Wuhan Xinxin Semiconductor Manufacturing Company, Wuhan, China
[3] College of Electronic Science and Engineering, Nanjing University of Posts and Telecommunications, Nanjing 210003, China

(Received 29 August 2016; revised manuscript received 26 September 2016; published online 30 November 2016)

We investigate the impact of random telegraph noise (RTN) on the threshold voltage of multi-level NOR flash memory. It is found that the threshold voltage variation ($\Delta V_{\rm th}$) and the distribution due to RTN increase with the programmed level ($V_{\rm th}$) of flash cells. The gate voltage dependence of RTN amplitude and the variability of RTN time constants suggest that the large RTN amplitude and distribution at the high program level is attributed to the charge trapping in the tunneling oxide layer induced by the high programming voltages. A three-dimensional TCAD simulation based on a percolation path model further reveals the contribution of those trapped charges to the threshold voltage variation and distribution in flash memory.

Keywords: random telegraph noise, NOR flash memory, percolation path, oxide charges

PACS: 85.30.De, 73.40.Qv, 85.40.Qx **DOI:** 10.1088/1674-1056/26/1/018502

1. Introduction

Random telegraph noise (RTN) has become a dominant noise source as the flash memory cell size scales down. It induces the cell threshold voltage ($V_{\rm th}$) shift and degrades the threshold voltage tight distribution during verification and read operation, which raises the possibility of failed bits.[1] Various aspects of the RTN phenomenon in flash cells have previously been analyzed.[2–5] In these works, the statistical distribution of RTN amplitude has been particularly studied due to its importance in determining RTN impact on the cell properties and program/erase (P/E) cycling reliability.[1,3–7] The research results illustrate that both the channel dopant fluctuation and the trap generation in the tunnel oxide layer aggravate the RTN impact on the cell's threshold voltage control.[8–19] On the other hand, RTN is a conspicuous issue for multi-level flash memory due to the stringent requirement of $V_{\rm th}$ distribution since multi-level cell program levels are closer to each other. Small RTN fluctuations could confuse the adjacent levels and lead to the errors of read operation. However, until now, there are few experimental reports about RTN characteristics on multi-level NOR flash memory.

In this paper, we studied the impact of random telegraph noise (RTN) on the threshold voltage of multi-level NOR flash memory. The RTN amplitude and distribution under different program levels ($V_{\rm th}$) and the read conditions are investigated and compared. The physical origin of the large RTN amplitude and wide distribution are attributed to the charge trapping in the tunneling oxide layer induced by the high programming voltages. Three-dimensional (3D) TCAD simulations were further introduced to illustrate the oxide trapping charge aggravation of $V_{\rm th}$ variation caused by RTN.

2. Experimental

The flash cells used in the study were fabricated in 90-nm NOR flash technology. They were programmed by channel hot electron (CHE) injection. The bias condition for gate/drain/source/bulk ($V_{\rm G}/V_{\rm D}/V_{\rm S}/V_{\rm B}$) is 7.1 V/3.8 V/0 V/0 V; by adjusting the programming time (t), multi-level storages were obtained. In order to separate the adjacent $V_{\rm th}$ distributions for meeting the minimum read margin, the distance between two adjacent programming levels is larger than 1 V. All electrical measurements in the study were conducted using a Keithley 4200 semiconductor characterization system on the Cascade Summit 12000 probe station.

RTN was evaluated by threshold voltage difference $\Delta V_{\rm th}$ between two subsequent read operations at a given programming level. Figure 1 shows two measured $I_{\rm D}$–$I_{\rm G}$ curves of the flash cell, here, $V_{\rm D}$ is fixed at 0.1 V. The initial $I_{\rm D}$–$I_{\rm G}$ curve is a smooth curve without RTN influence. It can be seen when a RTN event occurs at time t, the $I_{\rm D}$–$I_{\rm G}$ curve has a visible read current fluctuation, and then the channel current fluctuation $\Delta I_{\rm D}$ is monitored. Finally, the RTN amplitude $\Delta V_{\rm th}$ at time t can be extracted based on the equation of $\Delta I_{\rm D} = G_{\rm m}\Delta V_{\rm th}$. Here, $G_{\rm m}$ is trans-conductance under a given $V_{\rm G}$.

*Project supported by the National Research Program of China (Grant No. 2016YFB0400402), the Natural Science Foundation of Jiangsu Province, China (Grant No. BK20141321), and the National Natural Science Foundation of China (Grant No. 61627804).

†Corresponding author. E-mail: xji@nju.edu.cn

© 2017 Chinese Physical Society and IOP Publishing Ltd

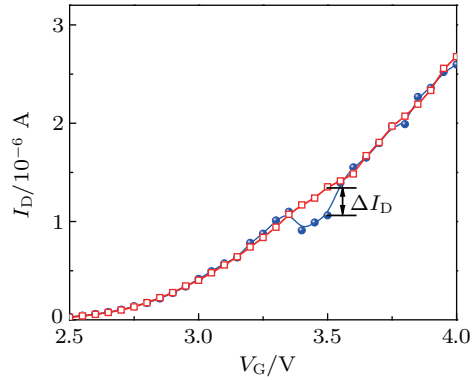


Fig. 1. (color online) The I_D–V_G curves for RTN amplitude (ΔV_{th}) extraction. Due to an electron trapped/de-trapped in the tunnel oxide trap, a RTN event may occur at time t and the value of ΔV_{th} can be extracted based on the equation of $\Delta I_D = G_m \Delta V_{th}$.

3. Results and discussion

According to the RTN measurement method mentioned above, we obtain the time traces of RTN amplitude (ΔV_{th}) with cell threshold voltage V_{th} varying from 3 V to 7 V, as shown in Fig. 2. It is seen that the program levels have an important influence on the properties of this RTN, including amplitude (ΔV_{th}), capture time (τ_c), and emission time (τ_e). With the increase of V_{th}, the ΔV_{th} is aggravated while the τ_c and τ_e become shorter and longer, respectively.

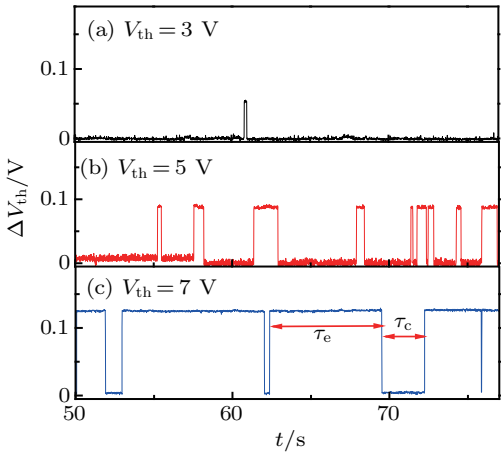


Fig. 2. (color online) Time trace of RTN amplitude (ΔV_{th}) at various program levels. To monitor RTN fluctuation, the read condition is set at $V_D = 0.1$ V and $V_G - V_{th} = 0.1$ V.

To gather RTN variability, several samples were measured and the complementary cumulative distribution function (1–CDF) of ΔV_{th} were calculated. Figure 3 shows RTN amplitude ΔV_{th} distributions at different V_{th} levels plotted on (1-CDF). It is found that the ΔV_{th} distribution is also highly dependent on the V_{th} levels. At high programming levels, there is a relatively larger ΔV_{th} distribution than that at low programming levels. At each programming level, the V_{th} dependence of ΔV_{th} appears approximately to have an exponential distribution:

$$1 - \mathrm{CDF} = \exp\left(-\frac{\Delta V_{th}}{\eta}\right). \quad (1)$$

Here, η represents the average value of the RTN amplitude.

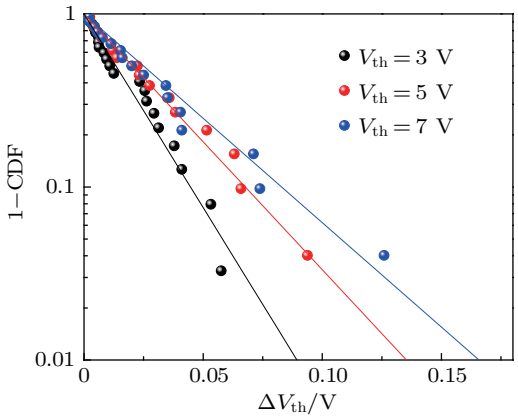


Fig. 3. (color online) RTN amplitude (ΔV_{th}) on the exponential plot. The solid lines present the fitting results with Eq. (1).

The obtained fitting parameters of η are about 22 mV, 29 mV, and 36 mV at the programming V_{th} levels of 3 V, 5 V, and 7 V, respectively. The strong program level dependence of η is clearly seen. The higher the program level is, the larger the RTN amplitude becomes. However, these fitting values are much larger than the theoretical calculation values by a simple charge sheet approximation model with an electron capturing in the tunnel oxide layer.[20] Similarly, it is also difficult to understand this tendency with a uniform flash cell model.

To correctly explain the abnormal large RTN fluctuation in the NOR flash memory devices, a non-uniform channel surface potential distribution model is proposed.[9,11] According to the quasi-two-dimensional Poisson equation, there is a surface non-uniformity potential distribution in the channel induced by the Si substrate random dopant distribution (RDD). However, the oxide charges trapping could also induce non-uniformity of potential profile in the channel, which will cause a large single RTN generation. In our study, the RTN average value is significantly increased with the program levels, therefore, we think that the oxide traps could be another reason for the non-uniform potential profile in the channel. Affected by the more fixed charges trapping in the oxide layer, the non-uniform potential distribution in the channel becomes much more obvious so that the channel currents could be divided into many narrow percolation paths. The RTN amplitude fluctuations at different program levels can be explained by the varying distance between the RTN trap position and the critical spot of the channel current path. When the RTN trap position is far from the critical spot of the channel percolation path, a smaller influence on the RTN characteristic is expected. However, when the RTN trap is just located above the critical spot of the percolation path, an abnormally large ΔV_{th} would be detected. The observed large ΔV_{th} (> 120 mV) at the program level of $V_{th} = 7$ V in Fig. 2 can be attributed to this obvious effect of the narrow percolation path in the channel.[9,10] Furthermore, the program-level dependency of ΔV_{th} in Fig. 3

strongly suggests that there exist various distances between RTN position and the narrow percolation paths.

The suggestion is further proved by the different V_G dependent tendency of ΔV_{th} at the various program levels. Figure 4 shows the ΔV_{th} values at various gate biases (V_G) for three program levels. It is observed that at the high program level of 7 V, the RTN fluctuation decreases with the increase of V_G. In contrast, the reverse tendency is observed at the low program levels of 3 V and 5 V. This experimental phenomenon is consistent with our hypothesis that the distances between the trap RTN location and the current percolation paths will have an important impact on RTN amplitude and distribution. When the program level of V_{th} is 7 V, the RTN trap may locate near the critical spot of the percolation path and block the current percolation path. As a result, a single RTN trap could induce the large ΔV_{th}. However, with the increase of gate bias V_G, the narrow percolation path in the channel could gradually become a wider integral path, and the abnormally large ΔV_{th} could gradually vanish due to the larger channel current. In contrast, when the program levels are 3 V and 5 V, the RTN trap may be far from the critical spot of the percolation path, consequently, the relatively smaller ΔV_{th} values are observed. Moreover, with the increase of gate bias V_G, the narrow percolation path gradually disappears, and the ΔV_{th} values are enhanced. This result also indicates that the distances between the RTN trap position and the narrow percolation paths could be changed under different program levels.

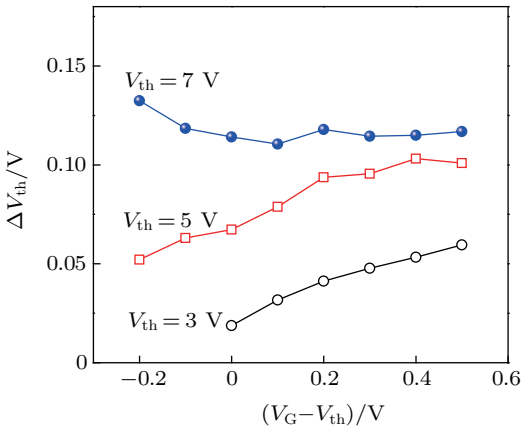


Fig. 4. (color online) The average ΔV_{th} with respect to the gate voltage (V_G) at various program levels.

As the position of the RTN trap is always fixed in the tunneling oxide, we consider this is attributed to the shift of the percolation paths under different program conditions. One possible explanation is the additional oxide traps near the Si/SiO_2 interface. According to the oxide trap model, more traps could be generated to capture charges under the programming condition with higher gate voltage.[21,22] More charges trapping in the tunnel oxide could induce the larger non-uniform potential distribution in the channel, which could result in more narrow percolation paths. Thus, the RTN trap locating near the critical spot of the percolation path may induce a large RTN. To further study the impact of additional charges in oxide on the RTN characteristic, we extracted average capture time (τ_c) and emission time (τ_e) of RTN. Figure 5 shows time constants dependence with the program levels of V_{th}. It can be found that τ_c shifts to the smaller value while τ_e shifts to the larger value as the program level increases. According to the field-assisted tunneling theory for capturing/emission electrons,[23–25] the above measured results strongly suggest that the oxide local field near the RTN trap is increasing with the program levels due to the new additional charges trapping in the tunnel oxide. Accordingly, the non-uniform potential distribution in the channel is enhanced with the increase of additional oxide charges. Although the increase of additional oxide traps can usually be observed during the P/E cycling process, the high program levels also can induce the degradation of tunnel oxide, which actually could be monitored sensitively by RTN fluctuation.

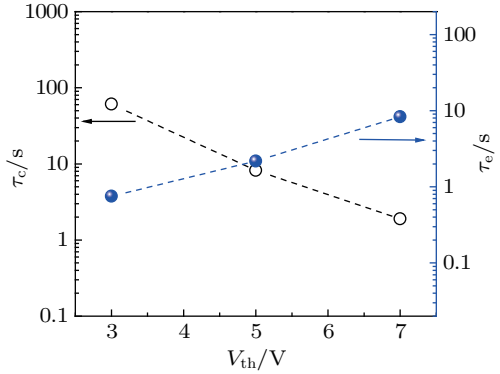


Fig. 5. (color online) The average capture time (τ_c) and emission time (τ_e) constants with respect to the program level (V_{th}).

4. TCAD simulation validation

To verify the proposed non-uniform channel surface potential distribution model, an accurate reproduction of the influence of generated trap charges on RTN amplitude was simulated using a channel surface potential model in combination with a percolation path by 3D Silvaco Atlas software. The channel length and width of the simulated flash cell are 130 nm and 80 nm, which are the same as those of the tested flash cell. The channel doping is calibrated by comparing the simulated and tested I_d–V_g characteristics of flash cell to improve the accuracy of TCAD simulation. In this simulation, a RTN trap is set at 0.1 nm away from the SiO_2/Si interface and then a number of fixed trap charges are randomly inserted in the oxide layer over the cell active area near the SiO_2/Si interface.

Figure 6 exhibits 3D simulation results of the channel potential shift $\Delta\phi$ with/without the fixed charges in the tunnel oxide layer from the initial one. It is clearly seen that the channel surface potential near the fixed oxide trap position is largely

changed. The more fixed charges in the tunneling oxide, the larger variation of the channel surface potential. This larger local potential shift will further have an important impact on the current percolation paths and the RTN characteristic of the devices.

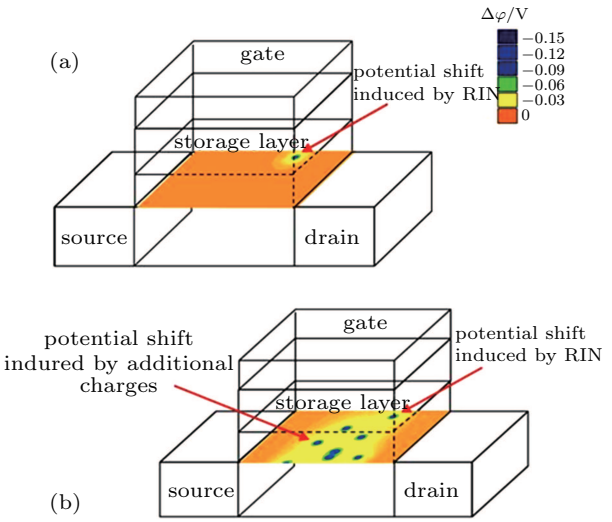


Fig. 6. (color online) The 3D TCAD simulation of the channel potential shift from the initial one when carriers are trapped by (a) RTN trap only; (b) RTN traps with additional fixed oxide traps. The channel surface potential near the fixed oxide trap position is largely changed. The more fixed charge in the tunneling oxide, the larger of the potential variation.

The simulated RTN amplitude is obtained by calculating $V_{\rm th}$ difference with and without the electron in a RTN trap. Figure 7 shows RTN magnitude $\Delta V_{\rm th}$ versus the number of fixed oxide charges. It is seen that $\Delta V_{\rm th}$ becomes evidently larger with the increase of charge number. Moreover, we can find that when there exists 0–4 fixed charges in the tunnel oxide, the RTN amplitude is enhanced with the increase of $V_{\rm G}$–$V_{\rm th}$, which may be attributed to the RTN trap position far from the current percolation paths. However, the reverse dependency is observed when the charges number in the tunnel oxide is increased from four to seven. In this case, the RTN trap position could be located near the critical spot of the percolation path. It is noted that the fixed oxide charges are increased with the program levels of $V_{\rm th}$, thus such $\Delta V_{\rm G}$–$V_{\rm th}$ dependency is very consistent with the experimental results in Fig. 4.

The generated fixed charges trapping in the tunnel oxide at high program levels not only induce the non-uniformity potential profile in the channel, but also have an impact on the local oxide electrical field. The inset of Fig. 7 shows the simulated oxide electrical field near the RTN trap at $V_{\rm G}$–$V_{\rm th} = 0.1$ V. It is seen that with the increase of charge number, the oxide field near the RTN trap increases. This is in good agreement with the characteristic of RTN $\tau_{\rm c}$ and $\tau_{\rm e}$ with the increase of program levels in Fig. 5.

Based on the experimental and TCAD simulation results, we can deduce that the more fixed charges captured in the tunneling oxide traps at the high program level could lead to the larger non-uniformity of potential profile in the channel, ultimately inducing the RTN aggravation of multi-level flash memory cells.

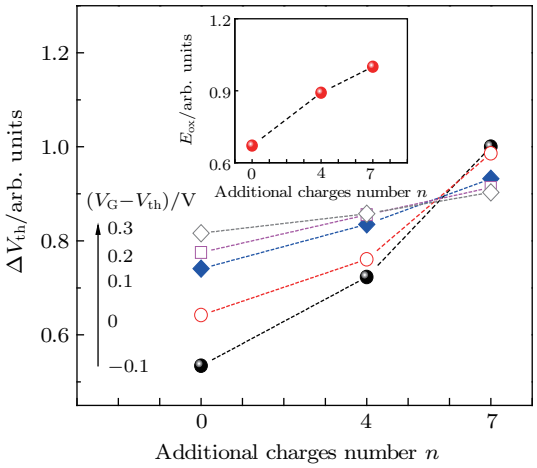


Fig. 7. (color online) Simulated $\Delta V_{\rm th}$ with respect to additional fixed oxide charge number. The inset shows the oxide field near RTN trap with respect to program levels.

5. Conclusion

The impacts of different $V_{\rm th}$ program levels on the RTN properties were comprehensively investigated in 90-nm NOR multi-level flash memories. It is found that the average value and variation of RTN amplitude $\Delta V_{\rm th}$ are significantly enlarged with the increase of program levels. The $\Delta V_{\rm th}$ is increased with $V_{\rm G}$ at the low program level while it exhibits the inverse tendency at the high program level. By means of 3D TCAD simulations, we can deduce that the generated traps in the tunneling oxide during the programming period could result in the serious non-uniformity of potential profile in the channel, which may be mainly responsible for the RTN aggravation at the high program level in the multi-level flash memories. A comprehensive treatment on RTN characterization, benchmarking, and usage should therefore comprehend such a discussion for advanced NOR flash cells.

References

[1] Gu S H, Li C W, Wang T, Lu W P, Chen K C, Ku J and Lu C Y 2006 *IEEE International Electron Devices Meeting (IEDM),* December 11–13, 2006, San Francisco, USA, p. 1

[2] Fukuda K, Shimizu Y, Amemiya K, Kamoshida M and Hu C 2007 *IEEE International Electron Devices Meeting (IEDM)*, December 10–12, 2007, Washington DC, USA, p. 169

[3] Joe S M, Yi J H, Park S K, Kwon H I and Lee J H 2010 *IEEE Electron Device Lett.* **37** 635

[4] Compagnoni C M, Castellani N, Mauri A, Spinelli A S and Lacaita A L 2012 *IEEE Trans. Electron Devices* **59** 2495

[5] Adamu-Lema F, Compagnoni C M, Amoroso S M, Castellani N, Gerrer L, Markov S, Spinelli A S, Lacaita A L and Asenov A 2013 *IEEE Trans. Electron Devices* **60** 833

[6] Veksler D, Bersuker G, Vandelli L, Padovani A, Larcher L, Muraviev A, Chakrabarti B, Vogel E, Gilmer D C and Kirsch P D 2013 *IEEE International Reliability Physics Symposium (IRPS)*, April 14–18, 2013, Monterey, USA, p. MY.10.1

[7] Ghetti A, Compagnoni C M, Spinelli A S and Visconti A 2009 *IEEE Trans. Electron Devices* **56** 1746
[8] Sonoda K, Ishikawa K, Eimori T and Tsuchiya O 2007 *IEEE Trans. Electron Devices* **54** 1918
[9] Franco J, Kaczer B, Toledano-Luque M, Roussel Ph J, Mitard J, Ragnarsson L Å, Witters L, Chiarella T, Togo M, Horiguchi N, Groeseneken G, Bukhori M F, Grasser T and Asenov A 2012 *IEEE International Reliability Physics Symposium (IRPS)*, April 15–19, 2012, Anaheim, USA, p. 5A.4.1
[10] Franco J, Kaczer B, Toledano-Luque M, Roussel Ph J and Groeseneken G 2013 *IEEE International Reliability Physics Symposium (IRPS)*, April 14–18, 2013, Monterey, USA, p. 2D.3.1
[11] Ma Z F, Zhuang Y Q, Du L and Wei S 2005 *Chin. Phys.* **14** 808
[12] Bae S H, Lee J H, Kwon H I, Ahn J R, Om J C, Park C H and Lee J H 2009 *IEEE Trans. Electron Devices* **56** 1624
[13] Aslam C A, Guan Y L and Cai K 2014 *Asia-pacific Signal & Information Processing Association, Summit & Conference (APSIPA)*, December 9–12, 2014, Chiang Mai, Thailand, p. 1
[14] Kurata H, Otsuga K, Kotabe A, Kajiyama S, Osabe T, Sasago Y, Narumi S, Tokami K, Kamohara S and Tsuchiya O 2007 *IEEE J. Solid-State Circuits* **42** 1362
[15] Tega N, Miki H, Osabe T, Kotabe A, Otsuga K, Kurata H, Kamohara S, Tokami K, Ikeda Y and Yamada R 2006 *IEEE International Electron Devices Meeting (IEDM),* December 11–13, 2006, San Francisco, USA, p. 1
[16] Amoroso S M, Ghetti A, Brown A R, Mauri A, Compagnoni C M and Asenov A 2012 *IEEE Trans. Electron Devices* **59** 2774
[17] Miccoli C, Paolucci G M, Compagnoni C M, Spinelli A S and Goda A 2015 *IEEE International Reliability Physics Symposium (IRPS)*, April 19–23, 2015, Monterey, USA, p. MY.9.1
[18] Chiu J P, Chou Y L, Ma H C, Wang T, Ku S H, Zou N K, Chen V, Lu W P, Chen K C and Lu C Y 2009 *IEEE International Electron Devices Meeting (IEDM)*, December 7–9, 2009, Baltimore, USA, p. 34.7.1
[19] Tega N, Miki H, Ren Z, D'Emic C P, Zhu Y, Frank D J, Cai J, Guillorn M A, Park D G, Haensch W and Torii K 2009 *IEEE International Electron Devices Meeting (IEDM)*, December 7–9, 2009, Baltimore, USA, p. 32.4.1
[20] Wolf S 1995 *Silicon Processing for the VLSI Era* (Vol. 3) (Sunset Bench: Lattice Press) pp. 89–98
[21] Waltl M, Goes W, Rott K, Reisinger H and Grasser T 2014 *IEEE International Reliability Physics Symposium (IRPS)*, June 1–5, 2014, Waikoloa, USA, p. XT.18.1
[22] Kimmel A V, Sushko P V, Shluger A L and Bersuker G 2009 *ECS Trans.* **19** 3
[23] Grasser T, Reisinger H, Wagner P J, Schanovsky F, Goes W and Kaczer B 2010 *IEEE International Reliability Physics Symposium (IRPS)*, May 2–6, 2010, Anaheim, USA, p. 16
[24] Grasser T, Kaczer B, Goes W, Aichinger Th, Hehenberger Ph and Nelhiebel M 2009 *IEEE International Reliability Physics Symposium (IRPS)*, April 26–30, 2009, Montreal, Canada, p. 33
[25] Ma Z F, Zhang P, Wu Y, Li W H, Zhuang Y Q and Du L 2010 *Chin. Phys. B* **19** 37201